

Improving the Spectral Resolution of HST Spectra via LSF Replacement

Steven V. Penton

*Center for Astrophysics and Space Astronomy, University of Colorado, Boulder,
CO 80309*

Abstract. Large aperture spectra provide greater signal, but small aperture spectra have higher resolution (smaller line-spread function (LSF) wings). The simple method presented here can convert large aperture spectra to the resolution of small aperture spectra by removing the wings of the LSF without significant noise being added to the continua. In addition, this method/algorithm allows spectra taken through different apertures to be placed upon a common baseline for increased signal-to-noise (S/N). In marginal S/N cases, such as QSO absorption studies, this method is a particularly promising archive mining tool.

1. Introduction

The method is inspired by the 2D ‘CLEAN’ method used in radio astronomy (Högbom, 1974), but adapted to 1D spectra. At the location of the highest flux point in the spectrum, a wavelength-dependent line-spread function (LSF) of photons is subtracted and its location stored. The LSF of photons subtracted is a small fraction ($< 10\%$) of the number of photons at this spectral location. Simultaneously, a new spectrum is created by adding a replacement LSF of photons at the original spectral location in the new spectrum. The replacement LSF could be a Gaussian of specified width, a delta-function, the LSF of another grating/aperture combination, or any other LSF (such as a ‘wingless’ approximation of the original or alternate LSF). Successive passes through the remaining spectrum result in a residual spectrum that, after many such passes, begins to resemble a featureless continuum. Iterations are truncated when the maximum remaining flux is a predetermined fraction of the original error vector, or, equivalently, when a certain size feature is no longer present in the spectrum. After this process has finished, a new spectrum is created by adding the remaining residual spectrum to the “cleaned” version.

2. Line-Spread Functions (LSFs)

The LSF describes the instrumental spectral distribution of an incident monochromatic emission source (delta-function) and is a function of aperture, grating, and wavelength. Sample HST/STIS first-order MAMA LSFs are shown in Figure 1 (taken from the STIS Instrument Handbook, Quijano et al. 2004). With increasing aperture size, and photon energy, the percentage of flux in the wings of the LSF increases significantly. HST spectral observers are forced to consider the trade-offs between apertures, often sacrificing flux (signal-to-noise) for resolution. For example, even though the reported literal full width half maximums (FWHM) are nearly identical, at 1200Å G140M observers were forced to select from apertures ranging from 42 to 91% transmissions and undocumented spectral resolution changes of greater than 20%.

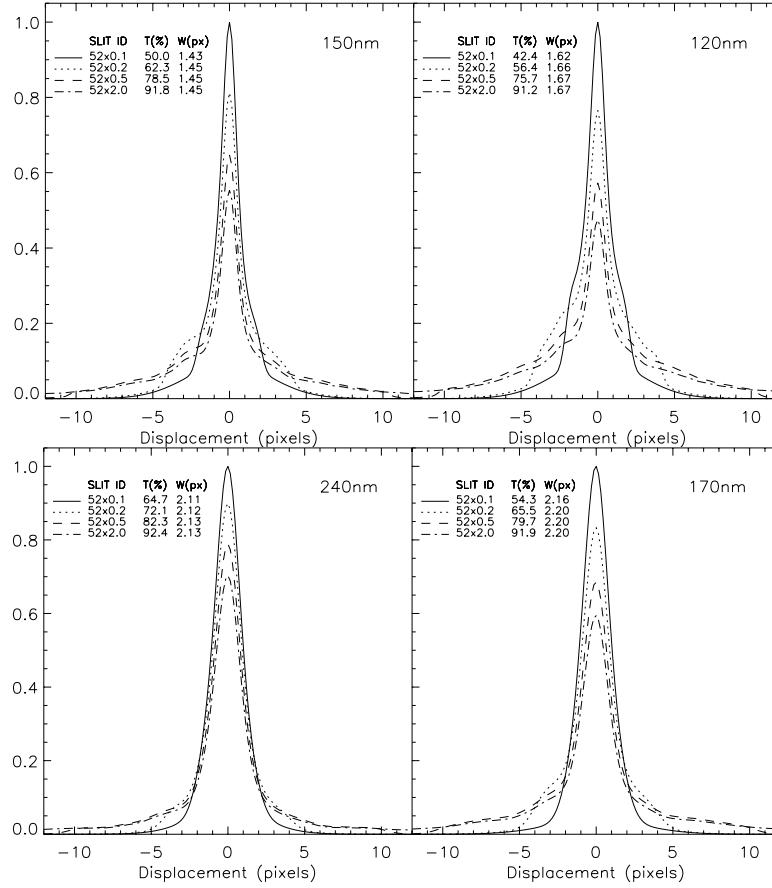


Figure 1: STIS first-order MAMA LSFs for the G140L and G140M (top) and G230L and G230M (bottom). The legend in the upper left gives the aperture, SLIT ID, the percentage of the incident flux transmitted by the aperture, $T(\%)$, and the FWHM of the central core in pixels, $W(\text{px})$. The wavelength is indicated in the upper right corner. The spectral method presented here is designed to increase spectral resolution by removing the significant, broad non-Gaussian wings.

3. Resolution Enhancement

Spectral resolution ($R=\lambda/\Delta\lambda$) is often defined by the literal FWHM of the central Gaussian core of a LSF and is only achievable for delta-function absorption or emission lines. To quantify the achievable resolution for a realistic astrophysical situation, we performed simulations with identical $b=20$ km/s (Doppler width, Penton et al. 2000) absorption features of variable separation at 1200\AA . We define the resolution R_{80} as the wavelength divided by the separation between identical Gaussian absorption features at which the central maxima between the two minima has a flux deficit of 80% of the feature minima. Sample simulations for two separations are shown in Figure 2.

We find the resolution (R_{80}) of STIS+G140M at 1200\AA to be $R_{80}\approx 5800$ ($\Delta\lambda=0.21\text{\AA}$) for the $52 \times 0.1''$ aperture and $R_{80}\approx 4500$ ($\Delta\lambda=0.27\text{\AA}$) for $52 \times 0.2''$. The ‘wingless’ $52 \times 0.1''$ replacement can resolve features at $R_{80}\approx 6500$ ($\Delta\lambda=0.18\text{\AA}$), and the delta-function replacement can resolve features at $R_{80}\approx 7700$ ($\Delta\lambda=0.16\text{\AA}$) (see Figure 3). This implies that we are able to increase STIS/G140M/ $52 \times 0.2''$ archive spectra from $R_{80}\approx 4500$ to 7700; a 71% improvement for our delta-function replacement, and a 46% improvement using the

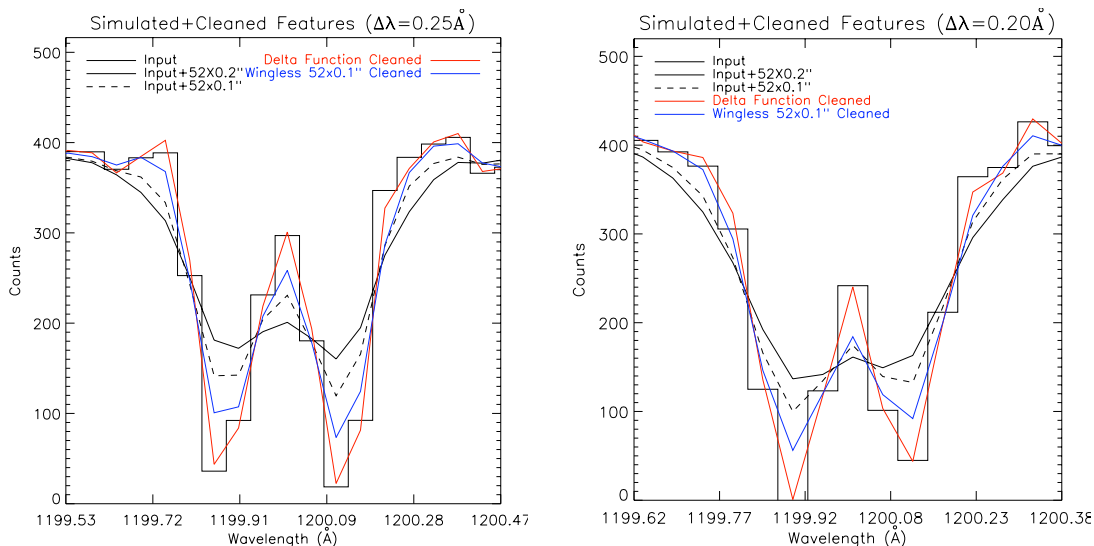


Figure 2: Left: A simulated S/N=20 per pixel STIS/G140M spectrum (rectangular contours) with $b=20$ km/s absorption features separated by 0.25\AA ($\Delta V \sim 60$ km/s) is convolved with the LSF of the $52 \times 0.2''$ aperture (minima ~ 170), then cleaned by two different methods (delta function: minima ~ 40 , wingless $52 \times 0.1''$: minima ~ 100). Shown for comparison is the convolution of the input spectrum with the $52 \times 0.1''$ LSF (dashed line). Both cleanings of the input $52 \times 0.2''$ spectra achieve improved resolution and are much better estimates of the known input spectrum. By our R80 definition, the input+ $52 \times 0.2''$ simulation does not resolve the features while the input+ $52 \times 0.1''$ and the cleaned spectra do. Right: For simulated/deconvolved spectral features separated by 0.2\AA ($\Delta V \sim 50$ km/s), neither of the original LSFs resolve the features, yet both spectral cleanings resolve the features.

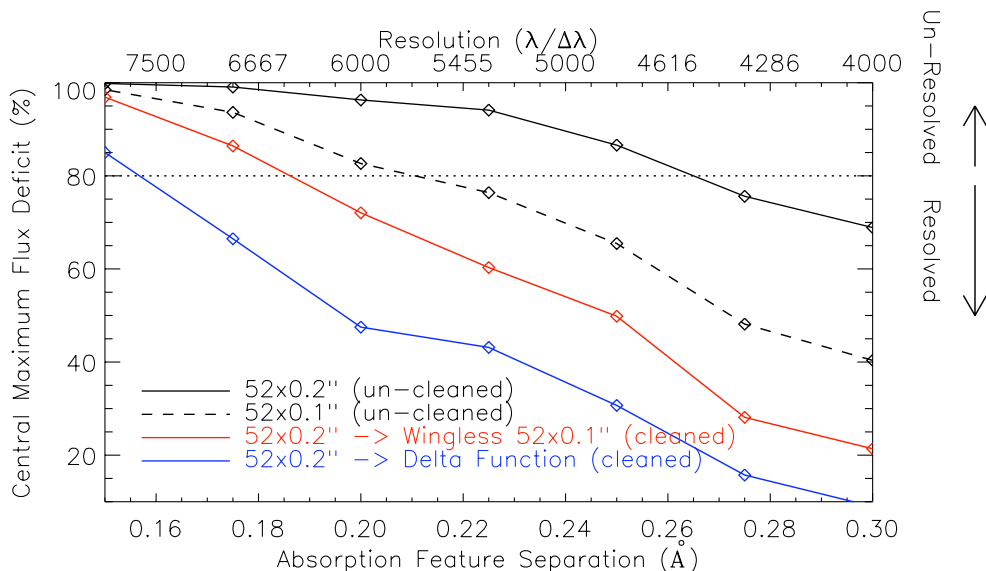


Figure 3: Simulation statistics (see Figure 2) allow us to calculate the relative resolutions of the G140M $52 \times 0.1''$ and $52 \times 0.2''$ apertures (upper solid and dashed lines) compared to spectral cleanings performed on simulated STIS/G140M/ $52 \times 0.2''$ data (lower solid lines). Our delta-function and ‘wingless’ $52 \times 0.1''$ ‘cleanings’ of input+ $52 \times 0.2''$ simulations achieve $\sim 70\%$ and $\sim 50\%$ higher spectral resolution than the input+ $52 \times 0.2''$ and input+ $52 \times 0.1''$ simulations, respectively.

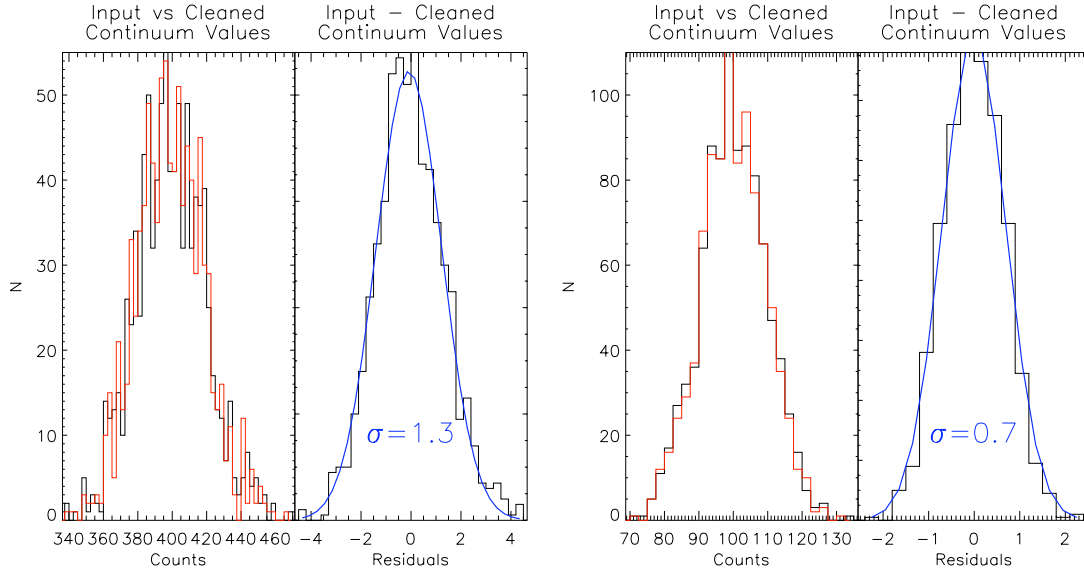


Figure 4: The left panel of the left figure shows the incident (black or dark) and delta-function-cleaned (red or light) continuum values for a simulated G140M 200 Å continuum region ($52 \times 0.2''$ aperture) with S/N per pixel of 20. The right panel of the left figure shows the pixel-to-pixel variations (residuals, black bar graph) between the input and cleaned continuum values. A Gaussian fit of the residuals (blue curve) demonstrates that the residuals appear mainly Gaussian with a σ of ± 1.3 counts or 0.3% ($1.3/400$). The right figure is identical, except that the S/N=10 per pixel, and the σ is ± 0.7 counts or 0.7% ($0.7/100$). In both examples, non-Gaussian excess residuals occur in $< 4\%$ of the cleaned continuum, and the excess is a small fraction of the intrinsic photon noise.

‘wingless’ $52 \times 0.1''$ replacement. We find similar results for low-resolution STIS spectra, but less dramatic results for echelle data, where the wings of the LSF are less pronounced.

4. Marginal (1%) Increase in Continuum Noise

To examine the effects of our spectral cleaning on continuum noise, we “cleaned” a simulated S/N of 20 (per pixel) STIS/G140M spectrum ($52 \times 0.2''$ aperture) over a continuum of 200 Å (4000 pixels, ~ 2600 resolution elements). The input spectrum, containing photon noise only, was convolved with the $52 \times 0.2''$ aperture LSF, then “cleaned” using a delta-function replacement. Figure 4 displays a histogram of the before and after continuum counts (left) and the differences (residuals, right) for a S/N of 20 simulated spectrum. We are able to retrieve the input spectrum with a $1\text{-}\sigma$ error of ± 1.3 counts, or $1.3/400 = 0.3\%$. For a S/N of 10 spectrum (right panel), we are able to retrieve the continuum to within 0.7%. In both examples, the non-Gaussian component of the residuals is $< 4\%$ and is a small fraction (20%) of the intrinsic photon noise. Further optimization of our algorithm will only reduce this non-Gaussian noise component. The main point is that even using the most extreme output LSF, a delta-function, the added non-Gaussian noise is quite small. This is, of course, a major concern since these non-Gaussian residuals could be misinterpreted as larger σ deviations and misidentified as real absorption or emission features.

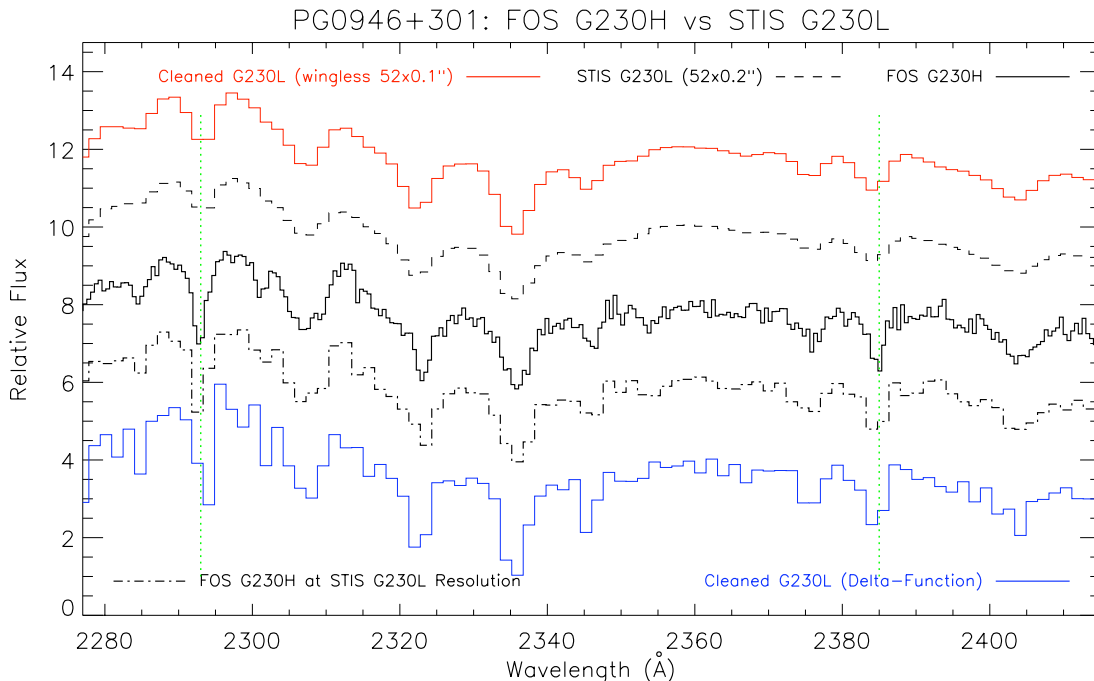


Figure 5: An HST/FOS spectrum of PG 0946+301 (G270H, central solid line) and a pipeline reduction of a similar resolution (G230L STIS, dashed line). Narrow absorption features $\text{Ly}\alpha$ at 2293\AA and 2383\AA are poorly reproduced by the normal STIS pipeline data reduction. Our spectral cleaning algorithm recovers the full extent of the absorption lines. The upper offset (red, top) spectrum is our ‘wingless’ $52 \times 0.1''$ LSF replacement, while the lower offset (blue, bottom) spectrum is our delta-function replacement. The dot-dashed line shows the FOS/G270H spectrum degraded to the STIS/G230L resolution.

5. HST Example

To demonstrate the operation of this algorithm we compare two spectral cleanings of HST/STIS/G230L/ $52 \times 0.2''$ observations of the QSO PG 0946+301 ($z = 1.216$) to the original spectrum and an HST/FOS/G270H spectrum (Figure 5). The two cleaned spectra (the ‘wingless’ $52 \times 0.1''$ and delta-function replacements) show deeper absorption features, more like the HST/FOS/G270H spectrum. In particular, narrow absorption features, such as $\text{Ly}\alpha$ at 2293\AA and 2383\AA , are poorly reproduced by the normal STIS pipeline data reduction, but are recovered by our spectral cleaning, which looks very similar to the FOS/G270H spectrum degraded to the STIS/G230L resolution.

6. Combining Spectra

At some level, all HST archival spectra should benefit from our spectral cleaning. However, of the 20,400 first-order STIS spectra in the archive, the $\sim 15,600$ (76%) that were taken with larger ($> 0.1''$) apertures will benefit the most from our spectral cleaning due to the significant LSF wings. Once “cleaned, these larger aperture datasets can be combined with other “cleaned” observations of the same target taken through other apertures without spectral degradation to produce higher signal-to-noise. In other words, this method allows archive users to place observations taken through different apertures onto a common frame. In addition, the negative impact of non-Gaussian wings of the LSF can be removed, resulting

in increased resolution with minimal contribution to continuum noise. Our algorithm works for all HST modes for which the LSF is well known.

7. Conclusions

By removing the non-Gaussian wings of the LSF, our algorithm increases the resolution of HST archive spectra by as much as 70% for the STIS medium resolution gratings, while introducing $< 1\%$ noise to the continuum. Our algorithm also allows spectra taken through different apertures to be combined in a way that actually increases the S/N and spectral resolution.

7.1. Caveats

- The algorithm only works if the LSF is well-known.
- This algorithm is ONLY designed to correct non-Gaussian LSF wings. If the intrinsic LSF does contain significant wings (i.e., HST/STIS echelle data), then this algorithm will not significantly improve the data, except in the case of combining data taken with different apertures.
- The algorithm is still under development and has not yet been applied to more than a couple of HST archive datasets. So, for now, one must consider this a promising, but unproven, calibration tool.
- There are several subtle nuances of the algorithm (which do not affect the statistics) that are not revealed here due to space limitations.
- Objects not centered in the aperture may have distorted LSFs, which cannot be corrected. This will result in decreased resolution improvement and increased continuum noise.

References

- Högbom, J. A. 1974, *A&AS*, 15, 417
Kim Quijano, J., et al. 2004, *STIS Instrument Handbook* (Baltimore: STScI)
Penton, S. V., Stocke, J. T., & Shull, J. M. 2000, *ApJS*, 130, 121